Synthesis and Thermal and Photoluminescence Properties of Liquid Crystalline Polyacetylenes Containing 4-Alkanyloxyphenyl trans-4-Alkylcyclohexanoate Side Groups

ARTICLE *in* MACROMOLECULES · JANUARY 2002

Impact Factor: 5.8 · DOI: 10.1021/ma0107962

3 AUTHORS, INCLUDING:

Jiun-Tai Chen
National Chiao Tung University
58 PUBLICATIONS **1,068** CITATIONS

SEE PROFILE

Synthesis and Thermal and Photoluminescence Properties of Liquid Crystalline Polyacetylenes Containing 4-Alkanyloxyphenyl *trans*-4-Alkylcyclohexanoate Side Groups

Ching-Hua Ting, Jiun-Tai Chen, and Chain-Shu Hsu*

Department of Applied Chemistry, National Chiao Tung University, Hsinchu, Taiwan, 30050, R.O.C.

Received May 7, 2001

ABSTRACT: Two series of polyacetylenes containing 4-alkanyloxyphenyl *trans*-4-*n*-alkylcyclohexanoate were synthesized using $[Rh(nbd)Cl]_2$, $MoCl_5$, and WCl_6 as initiators. Polymers **1P**−**3P**, which contain no flexible spacer, show no mesomorphic properties due to the rigid poly(phenylacetylene) backbone. Polymers **4P**−**9P**, which contain three or four methylene units in their spacers, exhibit both S_A and S_c phases. X-ray diffraction diagrams reveal that the liquid crystalline polyacetylenes display an interdigitated bilayer structure for the smectic phases. Polymers **4P**−**9P** are photoluminescent, and their emission wavelengths are about 500 nm. The photoluminescence intensity increased dramatically when a liquid crystalline polyacetylene was blended with poly(methyl methacrylate).

Introduction

Side-chain liquid crystalline polymers (SCLCPs) are of both theoretical and practical interest because they combine the anisotropic properties of liquid crystals with the polymeric properties and have potential application in the fields of nonlinear optics, optical data storage, piezoelectric transducer, and gas or liquid chromatography stationary phase.[1] So far, most SCLCPs have been based on flexible polymer backbones, such as polyacrylate, polymethacrylate, polysiloxane, and polyoxirane. Only a few rigid polymer backbones, such as polynorborane[2−14] and polyacetylene[15−19] have been used for the synthesis of SCLCPs because a rigid polymer backbone is believed to play a destructive role in the mesophase formation. Polyacetylene is the simplest class of conducting polymer. In 1993, Shirakawa et al. reported the first side-chain liquid crystalline polyacetylene prepared by Ziegler−Natta and methathesis initiators.[15] To form a liquid crystalline phase for the conducting polymer is the primary goal for introducing a mesogenic moiety as a substituted group in polyacetylene. The Japanese group successfully aligned the polymers with a magnetic field and found that the electrical conductivity of an aligned LC polyacetylene increased about 2 orders of magnitude in the direction parallel to the magnetic field.[16] The limitation on the synthesis of liquid crystalline polyacetylene is mainly due to the polar functional groups, which may poison the transition-metal initiators. Recently, Tang et al. developed a variety of functionality-tolerant and air and moisture-stable initiator systems and synthesized several series of side-chain LC polyacetylenes containing mesogens with ether, ester, amide and cyano functionalities.[20−24] Some of the side-chain LC polyacetylenes exhibit photoluminescent properties.[25−27] In our previous publications,[28,29] we reported several series of LC polysiloxanes and polyoxetanes containing 4-alkanyloxyphenyl *trans*-4-alkylcyclohexanoate side groups. These polymers reveal polymorphism of mesophases. In this study, polyacetylene was used as the polymer backbone. The effect of the polymer backbone on the mesomorphic properties of the obtained polymers is discussed. In addition, we report their photoluminescent properties.

Experimental Section

Materials. *trans*-4-*n*-Propylcyclohexanoic acid (99%), *trans*-4-*n*-butylcyclohexanoic acid (99%), and *trans*-4-*n*-pentylcyclohexanoic acid (99%) were obtained from Tokyo Chemical Inc. and were used as received. (Chloronorbornadiene)rhodium(I) dimer ($[Rh(nbd)Cl]_2$, 99%) was purchased from Strem. 4-Iodophenol (99%), 4-dichlorobis(triphenylphosphine)palladium(II) ($PdCl_2(PPh_3)_2$, 99.99%), copper(I) iodide (98%), triphenylphosphine (99%), 2-methyl-3-butyn-2-ol (98%), hydroquinone (99%), and 5-chloro-l-pentyne (98%) were purchased from Aldrich and used without further purification. Tetrahydrofuran (THF) was dried over sodium, and dioxane, triethylamine (Et_3N), and *N*,*N*-dimethylformamide (DMF) were dried over calcium hydride and then distilled under nitrogen.

Techniques. ^1H NMR spectra (300 MHz) were recorded on a Varian VXR-300 spectrometer. Thermal transitions and thermodynamic parameters were determined by using a Perkin-Elmer Pyris 1 differential scanning calorimeter equipped with a liquid nitrogen cooling accessory. Heating and cooling rates were 10 °C/min. A Carl-Zeiss Axiphot optical polarized microscope equipped with a Mettler FP82 hot stage and a FP80 central processor was used to observe the thermal transitions and to analyze the anisotropic textures. Gel permeation chromatography (GPC) was run on a Waters 510 LC instrument equipped with a 410 differential refractometer, a UV detector and a set of PL gel columns of 10^2, 5×10^2, 10^3, and 10^4 Å. The oven temperature was set at 40 °C. THF was used as eluent and the flow rate was 1 mL/min. The UV−visible spectra and photoluminescence of polymers were obtained from a Shimadzu UV-1601 spectrophotometer and an RF-5301PC spectrofluorophotometer, respectively.

Synthesis of Monomers 1M—9M. The synthesis of cyclohexane containing monomers **1M**−**9M** is outlined in Scheme 1.

4-(3-Hydroxy-3-methyl-1-butynyl)phenol (1). 4-Iodophenol (5.00 g, 22.7 mmol), $PdCl_2(PPh_3)_2$ (0.16 g, 0.23 mmol), CuI (0.22 g, 1.1 mmol), and PPh_3 (0.42 g, 1.6 mmol) were dissolved in triethylamine (150 mL), and the mixture was stirred under nitrogen. After all the catalysts were dissolved, 2-methyl-3-butyn-2-ol (2.30 g, 27.3 mmol) was added. The resulting solution was reacted at 70 °C for 15 h. After triethylamine was removed under reduced pressure, the product was extracted with diethyl ether. The crude product was isolated by

* Corresponding author.

10.1021/ma0107962 CCC: $22.00
Published on Web 01/12/2002

Scheme 1. Synthesis of Cyclohexane-Based Monomers 1M−9M

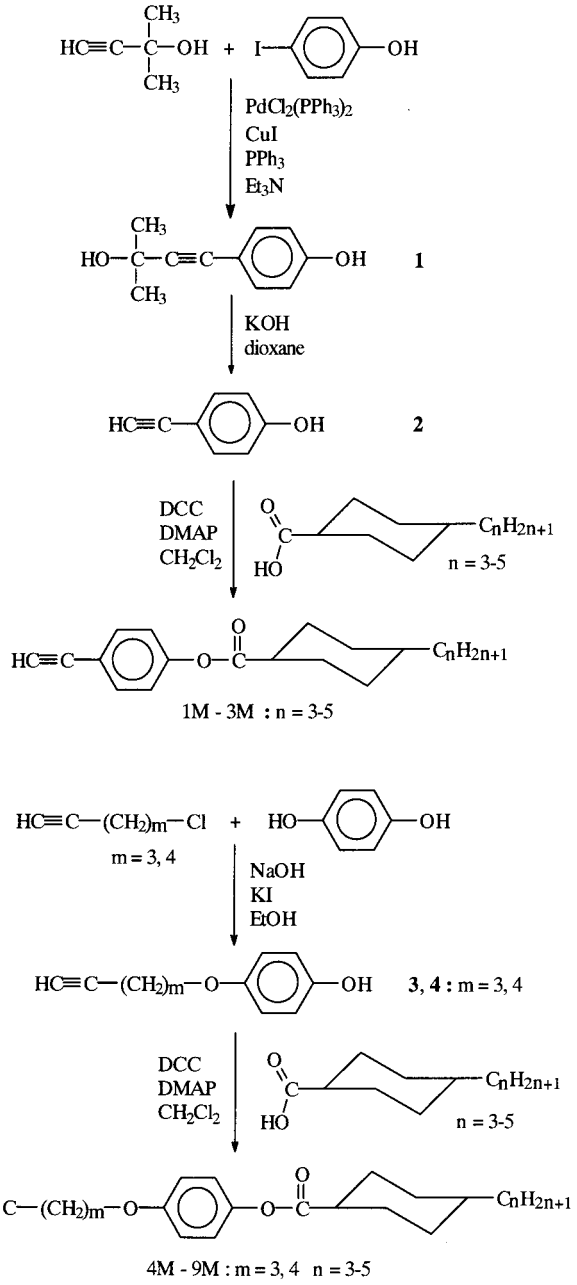

evaporating the solvent and purified by column chromatography (silica gel, ethyl acetate:*n*-hexane = 1:3 as eluent) and further recrystallized from methanol to yield 5.0 g (77%) of yellow crystals, mp = 123 °C. ^{1}H NMR ($CDCl_3$, δ, ppm): 1.59 (s, 6H, $-C(CH_3)_2-$), 6.76 and 7.26 (dd, 4H, aromatic protons).

4-(1-Ethynyl)phenol (2). 4-(3-Hydroxy-3-methyl-1-butynyl)phenol (3.00 g, 17.0 mmol) and KOH (2.10 g, 37.5 mmol) were dissolved in dioxane (100 mL). The mixture was reacted at 120 °C for 12 h. After the reaction system was cooled to room temperature, 6 N HCl aqueous solution (100 mL) was added. The mixture was extracted with ethyl ether. The crude product was isolated by evaporating the solvent and purified by column chromatography (silica gel, ethyl acetate:*n*-hexane = 1:1 as eluent) to yield 2.0 g (99%) of yellow crystals. ^{1}H NMR ($CDCl_3$, δ, ppm): 2.98 (s, 1H, $-C\equiv CH$), 6.76 and 7.36 (dd, 4H, aromatic protons).

4-(4-Pentynyloxy)phenol (3) and 4-(5-Hexynyloxy)-phenol (4). Both compounds were prepared by etherification of 5-chloro-1-pentyne or 6-chloro-1-hexyne with hydroquinone. The synthesis of compound **3** is described below.

Scheme 2. Synthesis of Side-Chain LC Polyacetylene 1P−9P

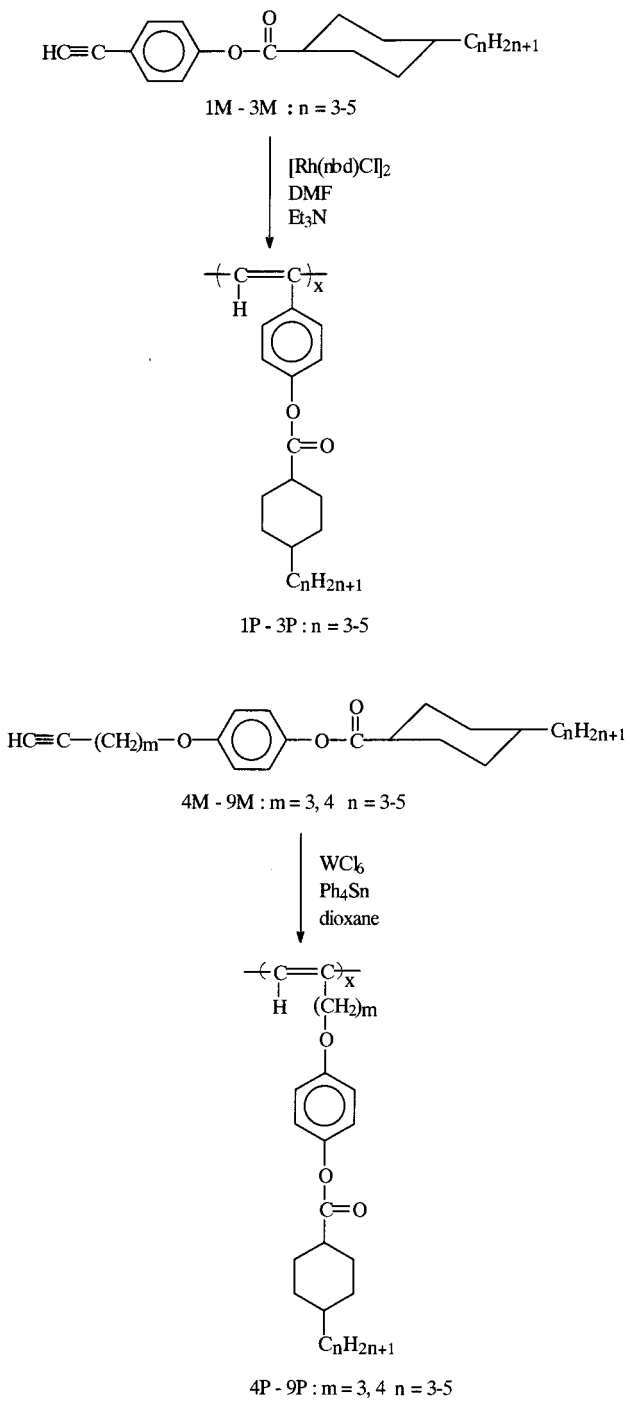

Hydroquinone (10.8 g, 97.5 mmol), NaOH (4.88 g, 122 mmol) and a catalytic amount of KI were dissolved in ethanol (150 mL) under gentle heating and stirring. Then 5-chloro-1-pentyne (5.00 g, 48.8 mmol) was added. The resulting mixture was heated to reflux temperature and stirred for 24 h. The solution was then poured into 350 mL of water and acidified with 20 mL of 37% HCl aqueous solution. The crude product which was isolated by filtration, was recrystallized from 96% methanol to yield 5.9 g (70%) yellow crystals, mp = 51.3 °C. ^{1}H NMR ($CDCl_3$, δ, ppm): 1.95 (s, 1H, $-C\equiv CH$), 1.96 (m, 2H, $-CH_2-$), 2.38 (m, 2H, $-CH_2-C\equiv$), 3.99 (t, 2H, $-OCH_2-$), 6.76 (dd, 4H, aromatic protons).

Compound **4**: yield 73%, mp = 74.5 °C. ^{1}H NMR ($CDCl_3$, δ, ppm): 1.70−1.85 (m, 4H, $-(CH_2)_2-$), 1.94 (s, 1H, $-C\equiv CH$), 2.25 (m, 2H, $-CH_2-C\equiv$), 3.90 (t, 2H, $-OCH_2-$), 6.75 (dd, 4H, aromatic protons).

Table 1. Characterization of Monomers 1M−9M

Monomer	Yield (%)	300 MHz 1H-NMR (CDCl$_3$, δ, ppm)
1M	75	0.87 (t, 3H, $-CH_3$), 0.90-2.16 (m, 13H, $-(CH_2)_2-CH<^{CH_2-CH_2-}_{CH_2-CH_2-}$), 2.46 (m, 1H, $-O-\overset{O}{\overset{\|}{C}}-CH<$), 3.03 (s, 1H, $HC\equiv C-$), 7.00 and 7.46 (dd, 4H, aromatic protons)
2M	68	0.89 (t, 3H, $-CH_3$), 0.90-2.15 (m, 15H, $-(CH_2)_3-CH<^{CH_2-CH_2-}_{CH_2-CH_2-}$), 2.46 (m, 1H, $-O-\overset{O}{\overset{\|}{C}}-CH<$), 3.03 (s, 1H, $HC\equiv C-$), 7.03 and 7.46 (dd, 4H, aromatic protons)
3M	50	0.87 (t, 3H, $-CH_3$), 0.90-2.15 (m, 17H, $-(CH_2)_4-CH<^{CH_2-CH_2-}_{CH_2-CH_2-}$), 2.46 (m, 1H, $-O-\overset{O}{\overset{\|}{C}}-CH<$), 3.03 (s, 1H, $HC\equiv C-$), 7.02 and 7.46 (dd, 4H, aromatic protons)
4M	65	0.87 (t, 3H, $-CH_3$), 1.94 (s, 1H, $HC\equiv C-$), 0.92-2.32 (m, 17H, $-C\equiv C-(CH_2)_2-$ and $-(CH_2)_2-CH<^{CH_2-CH_2-}_{CH_2-CH_2-}$), 2.43 (m, 1H, $-O-\overset{O}{\overset{\|}{C}}-CH<$), 4.02 (t, 2H, $-OCH_2-$), 6.87 and 6.92 (dd, 4H, aromatic protons)
5M	67	0.85 (t, 3H, $-CH_3$), 1.93 (s, 1H, $HC\equiv C-$), 0.92-2.32 (m, 19H, $-C\equiv C-(CH_2)_2-$ and $-(CH_2)_3-CH<^{CH_2-CH_2-}_{CH_2-CH_2-}$), 2.42 (m, 1H, $-O-\overset{O}{\overset{\|}{C}}-CH<$), 4.02 (t, 2H, $-OCH_2-$), 6.87 and 6.92 (dd, 4H, aromatic protons)
6M	73	0.87 (t, 3H, $-CH_3$), 1.95 (s, 1H, $HC\equiv C-$), 0.92-2.36 (m, 21H, $-C\equiv C-(CH_2)_2-$ and $-(CH_2)_4-CH<^{CH_2-CH_2-}_{CH_2-CH_2-}$), 2.46 (m, 1H, $-O-\overset{O}{\overset{\|}{C}}-CH<$), 4.03 (t, 2H, $-OCH_2-$), 6.87 and 6.93 (dd, 4H, aromatic protons)
7M	73	0.87 (t, 3H, $-CH_3$), 1.94 (s, 1H, $HC\equiv C-$), 0.91-2.33 (m, 19H, $-C\equiv C-(CH_2)_3-$ and $-(CH_2)_2-CH<^{CH_2-CH_2-}_{CH_2-CH_2-}$), 2.43 (m, 1H, $-O-\overset{O}{\overset{\|}{C}}-CH<$), 3.94 (t, 2H, $-OCH_2-$), 6.85 and 6.92 (dd, 4H, aromatic protons)
8M	73	0.86 (t, 3H, $-CH_3$), 1.95 (s, 1H, $HC\equiv C-$), 0.90-2.33 (m, 21H, $-C\equiv C-(CH_2)_3-$ and $-(CH_2)_3-CH<^{CH_2-CH_2-}_{CH_2-CH_2-}$), 2.43 (m, 1H, $-O-\overset{O}{\overset{\|}{C}}-CH<$), 3.94 (t, 2H, $-OCH_2-$), 6.85 and 6.92 (dd, 4H, aromatic protons)
9M	83	0.86 (t, 3H, $-CH_3$), 1.94 (s, 1H, $HC\equiv C-$), 0.90-2.32 (m, 23H, $-C\equiv C-(CH_2)_3-$ and $-(CH_2)_4-CH<^{CH_2-CH_2-}_{CH_2-CH_2-}$), 2.42 (m, 1H, $-O-\overset{O}{\overset{\|}{C}}-CH<$), 3.94 (t, 2H, $-OCH_2-$), 6.85 and 6.92 (dd, 4H, aromatic protons)

4-(1-Ethynyl)phenyl *trans*-4-*n*-alkylcyclohexanoate (1M—3M, *n* = 3—5), 4-(4-Pentynyloxy)phenyl *trans*-4-*n*-alkylcyclohexanoate (4M—6M, n = 3—5) and 4-(5-Hexynyloxy)phenyl trans-4-*n*-alkylcyclohexanoate (7M—9M, *n* = 3—5). Monomers **1M**−**9M** were synthesized by the same method. The preparation of monomer **2M** is described below.

Table 2. Thermal Transitions and Thermodynamic Parameters of Monomers 1M−9M

monomer	m^a	n^a	phase transitions, °C (corresponding enthalpy changes, kcal/mol):[b] heating/cooling
1M	0	3	K 79.2(4.78) I/I 63.9(0.08) N 32.1(4.42) K
2M	0	4	K 62.9(5.48) I/I 53.8(0.08) N 31.1(5.01) K
3M	0	5	K 63.4(7.37) N 87.5(0.14) I/I 86.6(0.11) N 46.1(7.27) K
4M	3	3	K 66.2(5.04) I/I56.3(0.05) N 48.3(4.08) K
5M	3	4	K 57.9(5.94) I/I 55.5(0.14) N 25.1(5.90) K
6M	3	5	K 66.2(4.70) N 71.3(0.12) I/I 70.8(0.15) N 44.3(4.95) K
7M	4	3	K 50.8(6.21) I/I 19.6(0.07) N 3.9(5.15) K
8M	4	4	K 48.3(8.52) I/I 23.4(0.08) N 2.5(7.00) K
9M	4	5	K 44.3(5.96) I/I 35(0.10) N 16.6(5.46) K

[a] According to Scheme 1. [b] K = crystalline, N = nematic, and I = isotropic. Data taken from the second heating and first cooling scan.

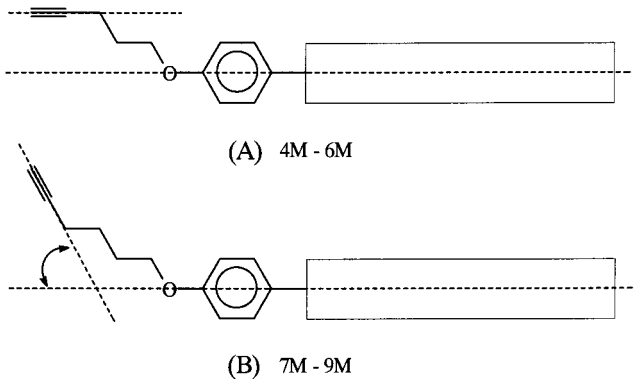

Figure 1. Structural configurations of LC acetylene derivatives with different spacer lengths: (A) three methylene units, and (B) four methylene units.

Table 3. Polymerization of 4-(1-Ethynyl)phenyl *trans*-4-*n*-Butylcyclohexanoate (2M)[a]

no.	initiator	solvent	reacn temp (°C)	yield (%)	$\overline{M_w} \times 10^{4}$ [b]	$\overline{M_w}/\overline{M_n}$ [b]
1	$MoCl_5/Ph_4Sn$	dioxane	rt[d]	0		
2	$MoCl_5/Ph_4Sn$	dioxane	80	0		
3	WCl_6/Ph_4Sn	dioxane	rt	0		
4	WCl_6/Ph_4Sn	dioxane	80	0		
5	$[Rh(nbd)Cl]_2$	THF	rt	49	27.4	2.2
6	$[Rh(nbd)Cl]_2$	$THF/Et_3N = 4:1$[c]	rt	56	17.3	4.3
7	$[Rh(nbd)Cl]_2$	$THF/Et_3N = 4:1$[c]	80	51	23.5	2.2
8	$[Rh(nbd)Cl]_2$	DMF	rt	80	13.6	5.2
9	$[Rh(nbd)Cl]_2$	$DMF/Et_3N = 4:1$[c]	rt	87	11.2	3.6
10	$[Rh(nbd)Cl]_2$	$DMF/Et_3N = 4:1$[c]	80	44	8.7	2.1

[a] Carried out under nitrogen for 24 h. $[M]_0 = 0.2$ M, $[[Rh(nbd)Cl]_2] = 10$ mM, $[WCl_6]$ $[MoCl_5] = [Ph_4Sn] = 20$ mM, nbd = 2,5-norborndiene, and Ph_4Sn = tetraphenyltin. [b] Determined by GPC in THF relative to polystyrene. [c] Volume ratio. [d] rt = room temperature.

trans-4-*n*-Butylcyclohexanoic acid (1.00 g, 5.87 mmol), 4-(1-ethynyl)phenol (1.00 g, 8.46 mmol) and *N*,*N*-dimethylaminopyridine (DMAP, 0.10 g, 0.85 mmol) were dissolved in dry CH_2Cl_2 (60 mL) under N_2 atmosphere. The solution was cooled to 0 °C, and dicyclohexyl carbodiimide (DCC, 2.10 g, 10.2 mmol) in 20 mL of dry CH_2Cl_2 was added dropwise. The reaction mixture was stirred at room temperature for 14 h and filtered. The crude product which was isolated by evaporating the solvent was purified by column chromatography (silica gel, ethyl acetate:*n*-hexane = 1:1 as eluent) and finally recrystallized from methanol to yield 1.2 g (68%) of yellow crystals, mp = 62.9 °C. ^{1}H NMR chemical shifts of monomers **1M**−**9M** are summarized in Table 1.

Polymerization of Monomers 1M—9M. Scheme 2 outlines the polymerization of monomers **1M**−**9M**. All polymerization reactions and manipulations were carried out under nitrogen using either an inert-atmosphere glovebox or Schlenk techniques in a vacuum line system, except for the purification of the polymers, which was done in an open atmosphere. An experimental procedure for the polymerization of monomer **6M** is given below.

Table 4. Polymerization of 4-(4-Pentynyloxy)phenyl *trans*-4-*n*-Pentylcyclohexanoate (6M)[a]

no.	initiator	solvent	reacn temp (°C)	yield (%)	$\overline{M_w} \times 10^{4}$ [b]	$\overline{M_w}/\overline{M_n}$ [b]
1	$MoCl_5$	dioxane	80	58	0.1	1.2
2	$MoCl_5/Ph_4Sn$	dioxane	80	70	0.3	1.9
3	$MoCl_5/Ph_4Sn$	toluene	80	65	1.5	1.2
4	WCl_6	dioxane	80	47	3.5	1.8
5	WCl_6/Ph_4Sn	dioxane	rt[d]	59	11.0	1.3
6	WCl_6/Ph_4Sn	dioxane	80	70	9.9	1.6
7	WCl_6/Ph_4Sn	toluene	rt	39	1.0	1.2
8	WCl_6/Ph_4Sn	toluene	80	75	2.0	1.2
9	$[Rh(nbd)Cl]_2$	$DMF/Et_3N = 4:1$[c]	rt	74	0.9	1.4
10	$[Rh(nbd)Cl]_2$	$DMF/Et_3N = 4:1$[c]	80	41	2.6	6.6

[a] Carried out under nitrogen for 24 h. $[M]_0 = 0.2$ M, $[[Rh(nbd)Cl]_2] = 10$ mM, $[WCl_6] = [MoCl_5] = [Ph_4Sn] = 20$ mM, $[Rh(nbd)Cl]_2 = 10$ mM, and nbd = 2,5-norborndiene. [b] Determined by GPC in THF relative to polystyrene. [c] Volume ratio. [d] rt = room temperature.

Table 5. Polymerization of Monomers 1M−9M[a]

M	initiator	solvent	reacn temp (°C)	yield (%)	$\overline{M_w} \times 10^{4}$[b]	$\overline{M_w}/\overline{M_n}$ [b]
1M	$[Rh(nbd)Cl]_2$	$DMF/Et_3N = 4:1$[c]	rt	78	8.3	4.4
2M	$[Rh(nbd)Cl]_2$	$DMF/Et_3N = 4:1$[c]	rt	87	11.2	3.6
3M	$[Rh(nbd)Cl]_2$	$DMF/Et_3N = 4:1$[c]	rt	72	9.6	3.7
4M	WCl_6/Ph_4Sn	dioxane	80	52	8.0	1.6
5M	WCl_6/Ph_4Sn	dioxane	80	55	7.9	1.9
6M	WCl_6/Ph_4Sn	dioxane	80	70	9.9	1.6
7M	WCl_6/Ph_4Sn	dioxane	80	60	7.8	1.4
8M	WCl_6/Ph_4Sn	dioxane	80	59	9.0	1.4
9M	WCl_6/Ph_4Sn	dioxane	80	70	14.5	1.6

[a] Polymerization takes place under nitrogen for 24 h. $[M]_0 = 0.2$ M, $[[Rh(nbd)Cl]_2] = 10$ mM, $[WCl_6] = [MoCl_5] = [Ph_4Sn] = 20$ mM, nbd = 2,5-norborndiene, DMF = dimethylformamide, Et_3N = triethylamine, and rt = room temperature. **M** = monomer. [b] Determined by GPC in THF relative to polystyrene. [c] Volume ratio.

Monomer **6M** (0.29 g, 0.80 mmol) was added into a Schlenk tube with a three-way stopcock on the sidearm. The tube was evacuated under vacuum and then flushed with dried N_2 three times through sidearm. Dioxane (2 mL) was injected into the tube through a septum to dissolve the monomer. The initiator solution was prepared in another tube by dissolving WCl_6 (31.7 mg, 0.08 mmol) and Ph_4Sn (34.2 mg, 0.08 mmol) in 2 mL of dried dioxane. Both tubes were aged at room temperature for 30 min. The monomer solution was then transfer to the initiator solution using a hypodermic syringe. The reaction mixture was stirred at 80 °C under N_2 for 24 h. The solution was then cooled to room temperature, diluted with 2 mL of THF and added dropwise to 300 mL of methanol through a cotton filter with stirring. The polymer was separated by filtration, purified by several reprecipitations from THF into methanol, and dried in a vacuum oven to yield 0.21 g (70%). $\overline{M_n} = 6.2 \times 10^4$, $\overline{M_w} = 9.9 \times 10^4$.

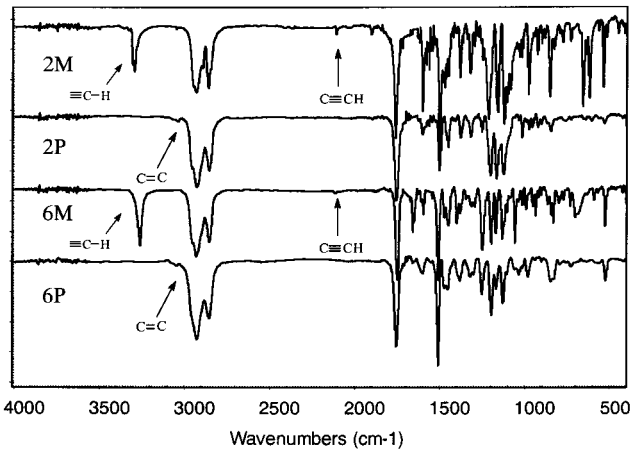

Figure 2. IR spectra of monomer **2M**, polymer **2P**, monomer **6M**, and polymer **6P**.

Preparation of Thin Films for Polymers 1P—9P and Blends of 9P and Poly(methyl methacrylate). The blends of polymer **9P** and poly(methyl methacrylate) (PMMA) were prepared by dissolution of both polymers in chlorobenzene. Polymers **1P**−**9P** and blends were spin-coated from chlorobenzene onto the cleaned quartz substrates. The solution concentration was 0.5 wt %. The spinning conditions were 1000 rpm/s for 10 s and 2000 rpm/s for 30 s.

Results and Discussion

Mesomorphism of Monomers 1M—9M. The thermal behavior of all monomers is reported in Table 2. Both monomers **3M** and **6M** reveal an enantiotropic nematic phase while all of the other monomers show only a monotropic nematic phase. The melting points decrease gradually as the spacer length (i.e., *m* value) increases. Among the first series of monomers **1M**−**3M**, which contain no methylene spacer, their melting points show an odd−even effect for the terminal alkyl group. This means that the melting point first decreases and then increases as the length of the terminal alkyl group increases. The odd−even effect is also observed in the second series of monomers **4M**−**6M**, which contain three methylene units in their spacers. Both monomers **3M** and **6M**, which contain a pentyl terminal group, show an enantiotropic nematic phase. This means that the longer alkyl terminal group stabilizes the nematic phase. However, in the third series of monomers **7M**−**9M**, which contain four methylene units in their spacers, all three monomers present only a monotropic nematic phase, and their melting points decrease as the length of the terminal alkyl group increases. Molecular simulation shows that the acetylene group of these monomers tilts away from the mesogenic core (Figure 1), which could be the reason for only a monotropic nematic phase.

Polymerization Reaction. Mo-, W-, and Rh-based compounds are the most widely used initiators for the polymerization of acetylene-based and phenylacetylene-based monomers.[15−24] Tang et al. found that $[Rh(nbd)Cl]_2$ can initiate polymerization of phenylacetylene-based monomers with cyano, ester and ether functionalities, but is not an effective initiator for the polymeri-

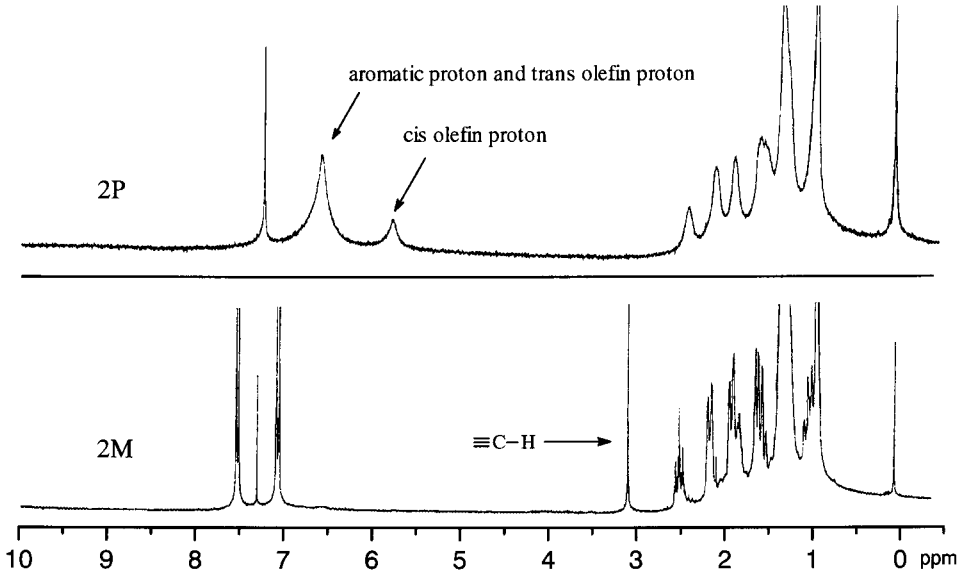

Figure 3. ^{1}H NMR spectra of monomer **2M** and polymer **2P**.

Table 6. Thermal Transitions of Liquid Crystalline Polyacetylenes 1P−9P

polymer	m^a	n^a	cis content (%)[b]	phase transitions, °C (corresponding enthalpy changes, kcal/mol)[c] heating/cooling
1P	0	3	84	170 (isomerization)[d]
2P	0	4	88	185 (isomerization)[d]
3P	0	5	84	189 (isomerization)[d]
4P	3	3	0	G 57 S_x 138(0.19) S_A 165(0.85) I/I 161(0.81) S_A 135(0.09) S_x
5P	3	4	0	G 59 S_x 148(0.23) S_A 181(0.91) I/I 175(0.79) S_A 144(0.11) S_x
6P	3	5	0	G 69 S_x 166(0.18) S_A 194(0.82) I/I 189(0.77) S_A 160(0.10) S_x
7P	4	3	0	G 54 S_x 119(0.23) S_A 148(0.81) I/I 144(0.80) S_A 115(0.10) S_x
8P	4	4	0	G 63 S_x 119(0.21) S_A 151(0.79) I/I 147(0.76) S_A 117(0.09) S_x
9P	4	5	0	G 63 S_x 126(0.19) S_A 176(0.70) I/I 174(0.66) S_A 120(0.11) S_x

[a] According to Scheme 1. [b] Determined by ^{1}H NMR spectra. [c] G = glassy, S = smectic, I = isotropic. Data taken from the second heating and first cooling scan. [d] Data taken from the first heating scan.

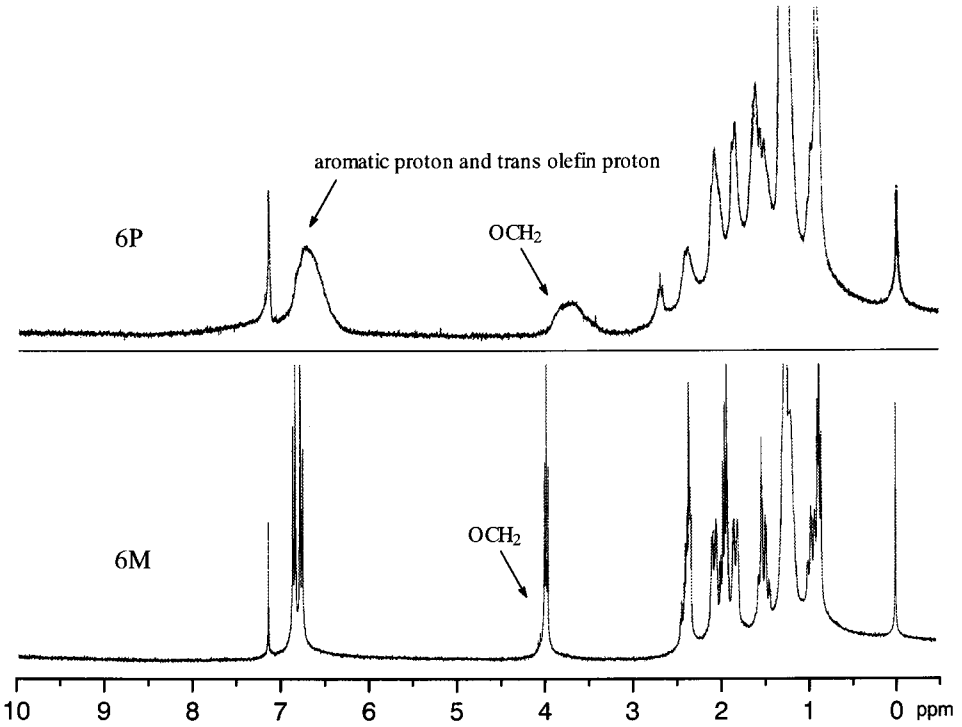

Figure 4. ^{1}H NMR spectra of monomer **6M** and polymer **6P**.

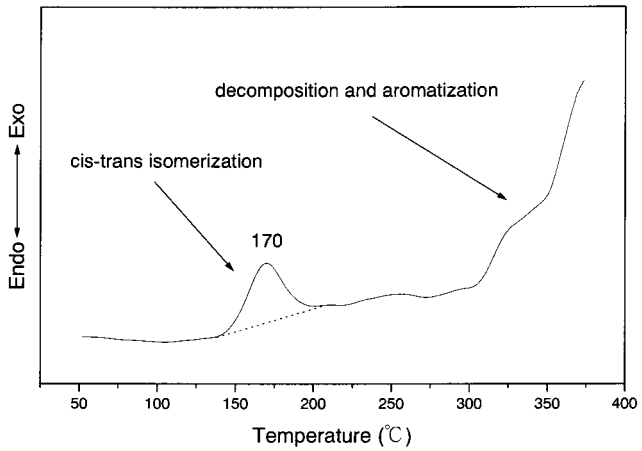

Figure 5. DSC thermogram of polymer **1P** (10 °C/min): the first heating scan.

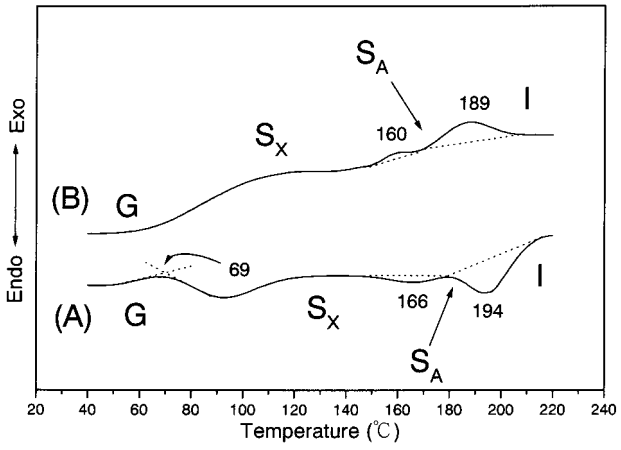

Figure 6. DSC thermograms of polymer **6P** (10 °C/min): (A) heating scan and (B) cooling scan.

zation of acetylene-based monomers.[23] They also found that WCl_6-Ph_4Sn is the best initiating system for the polymerization of acetylene-based monomers with polar functionalities.[21] In this study, monomers **1M**−**3M** belong to phenylacetylene-based monomers while monomers **4M**−**9M** are acetylene-based monomers. Therefore, we chose WCl_6, $MoCl_5$, and $[Rh(nbd)Cl]_2$ as initiators and Ph_4Sn as a co-initiator. Table 3 lists the polymerization results of monomer **2M**. Neither WCl_6-Ph_4Sn nor $MoCl_5-Ph_4Sn$ initiate the polymerization of monomer **2M**, while $[Rh(nbd)Cl]_2$ gives polymers with reasonably high yields and molecular weights in all cases. The yields are around 50% when THF or a mixture of THF and Et_3N are used as solvent. When the solvent is changed from THF to DMF, the yield at room temperature is improved but the $\overline{M_w}$ value decreases. The addition of Et_3N to DMF improves the yield at room temperature slightly. When the polymerization temperature is raised to 80 °C, the yield largely decreases for the DMF/Et_3N solvent system. The best polymerization conditions for monomer **2M** use (i) $[Rh(nbd)Cl]_2$ as initiator, (ii) a mixture of DMF and Et_3N (4:1, volume ratio) as solvent, and (iii) polymerization at room temperature. Table 4 reports the polymerization results of monomer **6M**. $MoCl_5$ alone in dioxane gives only oligomers. When Ph_4Sn is used as co-initiator, the molecular weights increase slightly ($\overline{M_w}$ = 3430). For the same $MoCl_5-Ph_4Sn$ initiating system, changing the solvent from dioxane to toluene, increases the weight average molecular weights to 14600. WCl_6 alone in dioxane gives polymers with reasonably high molecular weight and moderate yield (47%). When Ph_4Sn is used as co-initiator, both the molecular weight and yield increase. For the same WCl_6-Ph_4Sn initiating system, the solvent changing from dioxane to toluene, increases the yield, but largely decreases the average molecular weight. As far as the polymerization temperature, better polymerization results are obtained at 80 °C than at room temperature.

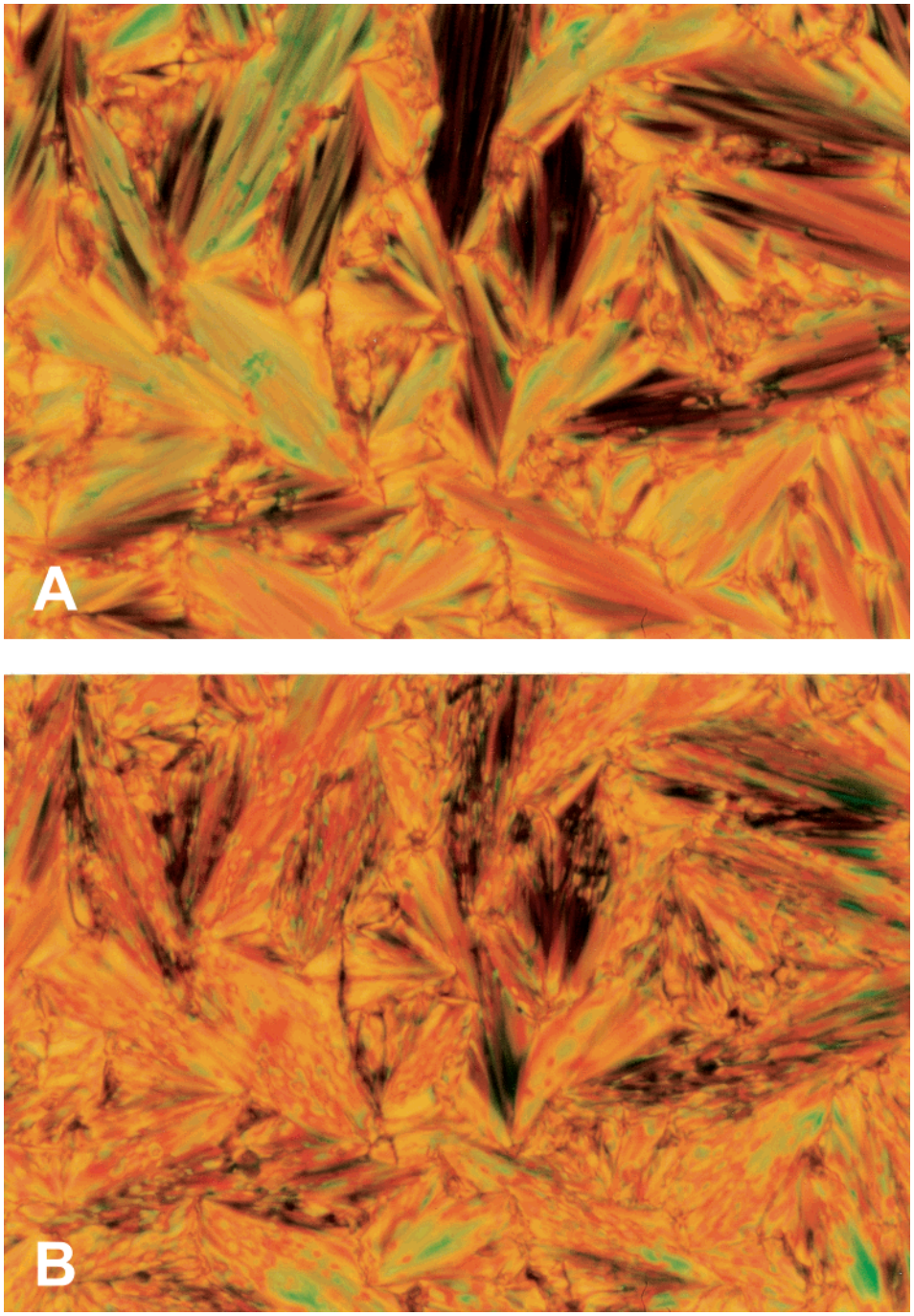

Figure 7. Polarizing optical micrographs displayed by polymer **6P**: (A) focal−conic fan texture of the smectic A phase obtained after cooling from the isotropic melt to 170 °C; (B) broken fan texture of the smectic phase obtained after cooling from the isotropic melt to 100 °C.

Although $[Rh(nbd)Cl]_2$ gives polymers with high yield at room temperature, the weight average molecular weight is quite low ($\overline{M_w}$ = 9030). When the polymerization temperature is raised to 80 °C, the molecular weight increases slightly, but the yield decreases dramatically. The best polymerization conditions for monomer **6M** use (i) WCl_6-Ph_4Sn as initiating system, (ii) dioxane as solvent, and (iii) polymerization at 80 °C.

Table 5 reports the polymerization results of monomers **1M**−**9M**. Monomers **1M**−**3M** were polymerized by $[Rh(nbd)Cl]_2$ in a mixture of DMF and Et_3N at room temperature, while monomers **4M**−**9M** were polymerized by WCl_6-Ph_4Sn in dioxane at 80 °C. All polymerizations give polymers with reasonably high yields and molecular weights.

Structure Characterization of Polymers 1P—9P. Figure 2 compares the IR spectra of monomer **2M** and **6M** with those of their corresponding polymers **2P** and **6P**. Both monomers absorb at about 3260 and 2100 cm^{-1}, due respectively to the C≡C stretching and ≡C−H stretching vibrations. Both acetylene absorption bands disappear in the spectra of the polymers. A new double bond absorption at 3050 cm^{-1} appears in the polymer spectra, confirming that acetylene triple bonds have been converted to conjugated double bonds during the polymerization.

Figure 3 shows the ^1H NMR spectra of monomer **2M** and polymer **2P**. In the spectrum of polymer **2P**, the acetylene proton peak at 3.03 ppm disappears and two new broad peaks appear at 5.77 and 6.60 ppm. Simi-

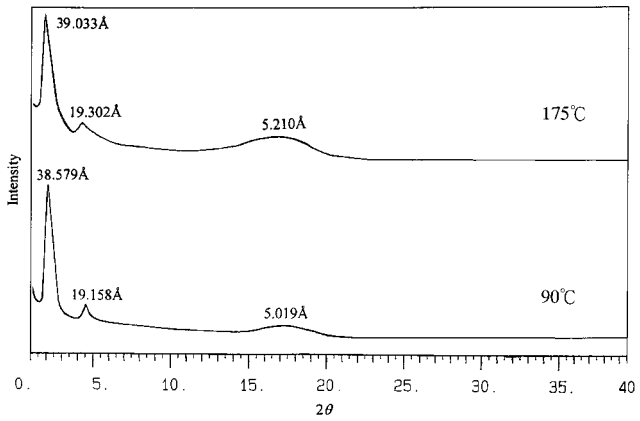

Figure 8. X-ray diffraction patterns of polymer **6P** measured after cooling from the isotropic melt to 175 and 90 °C.

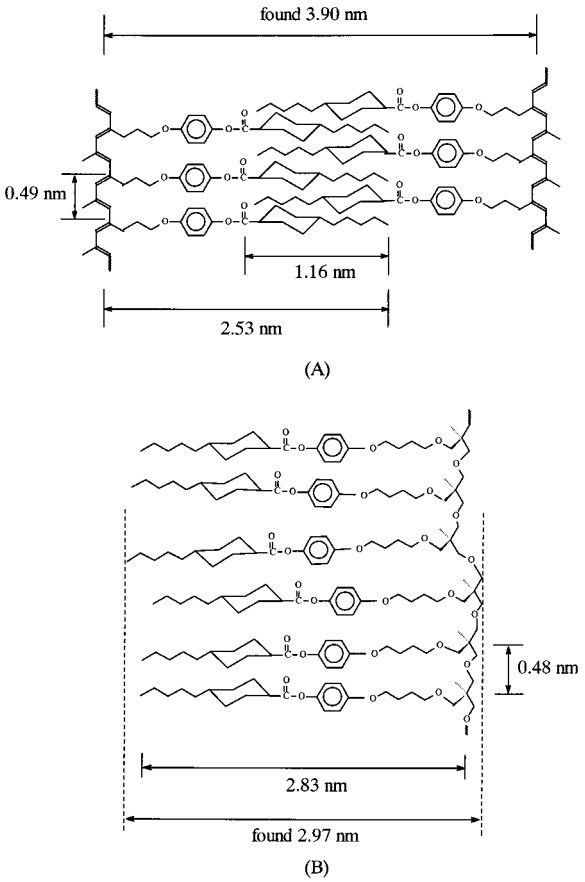

Figure 9. Smectic layer structures of (A) polyacetylene, and (B) polyoxetane.

onesue and Percec.[30,31] have reported that the *cis*-olefin proton peak appears at 5.82 ppm and *trans*-olefin proton peak appears at 6.85 ppm for poly(phenylacetylene). Therefore, we can calculate the cis content of a polymer by the following equation:

$$\text{cis content (\%)} = \{A_{5.77}/[(A_{5.77} + A_{6.60})/5]\} \times 100$$

The cis contents of polymers **1P**, **2P**, and **3P** are 84, 88, and 84% respectively. Figure 4 presents the ^{1}H NMR spectra of monomer **6M** and polymer **6P**. In the spectra of **6P**, only a broad peak at 6.85 ppm is observed in the region from 5 to 7 ppm. According to Tang et al.,[21] the chemical shift of *cis*-olefin proton appear in the region 5.88−6.26 ppm for mesogen-containing poly(1-alkynes).

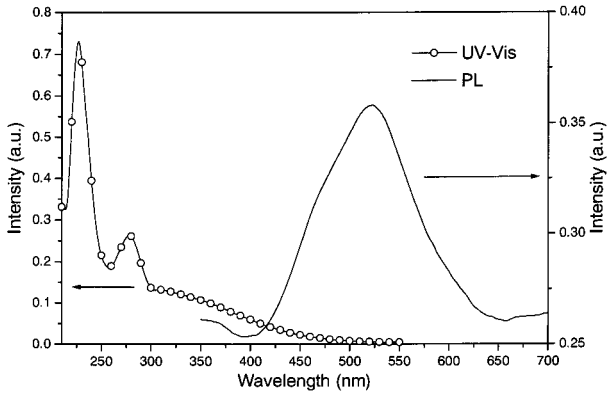

Figure 10. UV−visible and photoluminescence spectra of polymer **9P**.

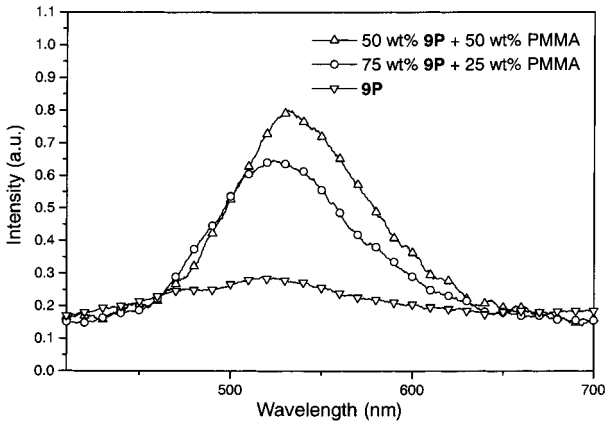

Figure 11. Photoluminescence spectra of polymer **9P** and its mixtures with PMMA.

Table 7. UV−Visible and Photoluminescent Data of Polymers 1P−9P'

	UV−visible[a]		photoluminescence[b]	
polymer	λ_{abs} (nm)		λ_{ex} (nm)	λ_{em} (nm)
1P	394	331	393	
2P	396	330	395	
3P	396	326	396	
4P	278	227	278	515
5P	279	226	278	488
6P	279	228	278	478
7P	280	226	279	500
8P	279	227	279	485
9P	280	227	279	519

[a] Code: λ_{abs}, absorptive wavelength in UV−visible spectrum. [b] Code: λ_{ex}, exciting wavelength used in the measurement of photoluminescence; λ_{em}, emissive wavelength in photoluminescence spectrum.

No peak is observed in this region for polymer **6P**. Therefore we conclude that the *trans*-olefin content of polymer **6P** is 100%. The same is true for polymers **4P**, **5P**, and **7P**−**9P**.

Mesomorphic Properties of Polymers 1P—9P. Table 6 summarizes the phase transitions of polymers **1P**−**9P**. Polymers **1P**−**3P** show no mesophase while polymers **4P**−**9P** reveal two enantiotropic smectic phases. Figure 5 displays a representative DSC trace of polymer **1P**. It exhibits a cis−trans isomerization peak at 170 °C. The cis−trans isomerization was checked by ^{1}H NMR. After polymer **1P** was annealed at 250 °C for 10 min, the chemical shift of the *cis*-olefin at 5.77 ppm disappeared and the chemical shift of the *trans*-olefin was supposed to form at about 7.0 ppm.

However, it overlapped with the aromatic protons. Similar result was reported by Matsunami et al.[32] Since polymer **1P** has a very rigid polyacetylene backbone and contains no spacer, it is very difficult for the mesogenic side groups to form a mesophase. Polymer **1P** underwent decomposition and other aromatization side reaction at over 300 °C, which agrees with the thermogravimetry measurement.

Figure 6 presents representative DSC thermograms of polymer **6P**. It displays two smectic phases on both heating and cooling scans. The mesophase identification have been achieved by optical polarizing microscopic observation and X-ray diffraction. Figure 7A shows a focal−conic fan, and Figure 7B shows a broken fan textures exhibited by polymer **6P**. Figure 8 presents the temperature-dependent X-ray diffraction diagrams obtained from powder samples of **6P** at 175 and 90 °C. At 175 °C, the diffraction diagram presents a diffuse reflection at 5.21 Å, which corresponds to the lateral spacing of two mesogenic side groups, and a sharp first-order reflection at 39.03 Å and a second-order reflection at 19.30 Å, which correspond to smectic layers. The optical polarizing micrograph reveals a focal-conic fan texture at this temperature range. Both results are consistent with a smectic A structure. When the measuring temperature is lowered from 175 to 90 °C, the *d* spacing of the first-order reflection decreases from 39.03 to 38.58 Å. The optical polarizing micrograph (Figure 7B) shows a broken fan texture at this temperature range. The results indicate the formation of a tilted smectic phase, probably a smectic C phase. The detailed structure of the smectic phase showed be further studied by X-ray diffraction pattern of an aligned monodomain sample.

Comparison of the Effect of Rigid and Flexible Polymer Backbones on Their Mesomorphic Properties. Since polyacetylene is a very rigid polymer backbone, we can investigate the effect of a rigid polymer backbone on their mesomorphic properties. In a previous publication,[29] we reported a series of polyoxetanes containing the same 4-alkanyloxyphenyl *trans*-4-alkylcyclohexanoate side groups. The polyacetylenes synthesized in this study have much higher glass transition and isotropization temperatures than the corresponding polyoxetanes. The reason could be due to the rigidity of the polyacetylene backbones. As far as the mesomorphic behavior, polymers **4P**−**9P** reveal smectic A and smectic C phases, while the polyoxetanes display a nematic phase and two smectic phases. The LC polymers with rigid polymer backbones have a tendency to form smectic phases. The *d* spacing of smectic layer for LC polyacetylene is 39.03 Å at 175 °C. According to molecular calculation, the layer spacing is considerably greater than molecular length of the side group in a LC polyacetylene. The LC polyacetylenes obviously tend to form an interdigitated bilayer structure (Figure 9A). According to our previous report,[29] the smectic layer spacing of a LC polyoxetane is about 29.7 Å which is very close to the molecular length of its side groups. Thus, the LC polyoxetane which contain a more flexible backbone form only the single layer smectic arrangement (Figure 9B).

Photoluminescent Properties of Polymers 1P—9P. Table 7 summarizes the results of UV−vis and photoluminescent spectra of polymers **1P**−**9P**. Polymers **1P**−**3P** exhibit two UV−vis absorption peaks at about 330 and 395 nm and show no photoluminescent property at all. However, polymers **4P**−**9P** present two UV−vis absorption peaks at about 226 and 279 nm and emit a luminescence peak at 500 nm. Figure 10 shows the representative UV−vis and photoluminescent spectra of polymer **9P**. The photoluminescent intensity of polymer **9P** is quite weak due to strong intermolecular interactions which give rise to self-quenching. Nevertheless, when **9P** was blended with PMMA, its photoluminescent intensity increases dramatically (Figure ll). The photoluminescent intensity increases as the weight percentage of PMMA increases from 25 to 50. The results demonstrate that the addition of a nonemissive polymer as diluent for the LC polyacetylene reduces its interchain interaction and therefore enhances its photoluminescent intensity.

Conclusion

A new series of side-chain LC polyacetylenes containing 4-alkanyloxyphenyl *trans*-4-alkylcyclohexanoate side groups were synthesized using simple metal halide initiators. Polymers **1P**−**3P** without flexible spacer, show no mesomorphic behavior, while polymers **4P**−**9P** containing three or four methylene units in their spacers, display both smectic A and smectic C phases. Compared to the corresponding polyoxetanes, the LC polyacetylenes have much higher glass transition and isotropization temperatures. X-ray diffraction results also demonstrate that the LC polyacetylenes tend to form an interdigitated bilayer structure for the smectic phases. Polymers **4P**−**9P** have a weak photoluminescence emission at about 500 nm. After blending with PMMA, their photoluminescence intensities increase dramatically.

Acknowledgment. The authors are grateful to the National Science Council of the Republic of China for financial support of this work (NSC 89-2216-E009-023).

References and Notes

(1) Hsu, C. S. *Prog. Polym. Sci.* **1997**, *22*, 829.
(2) Komiya, Z.; Pugh, C.; Schrock, R. R. *Macromolecules* **1992**, *25*, 6586.
(3) Pugh, C.; Schrock, R. R. *Macromolecules* **1992**, *25*, 6593.
(4) Komiya, Z.; Schrock, R. R. *Macromolecules* **1993**, *26*, 1387.
(5) Komiya, Z.; Schrock, R. R. *Macromolecules* **1993**, *26*, 1393.
(6) Kim, S. H.; Lee, H. J.; Jin, S. H.; Cho, H. N.; Choi, S. K. *Macromolecules* **1993**, *26*, 846.
(7) Pugh, C. *Macromol. Symp.* **1994**, *77*, 325.
(8) Ungerank, M.; Winkler, B.; Eder, E.; Stelzer, F. *Macromol. Chem. Phys.* **1995**, *196*, 3623.
(9) Pugh, C.; Liu, H.; Arehart, S. V.; Narayanan, R. *Macromol. Symp.* **1995**, *98*, 293.
(10) Maughon, B. R.; Weck, M.; Mohr, B.; Grubbs, R. H. *Macromolecules* **1997**, *30*, 257.
(11) Pugh, C.; Dharia, J.; Arehart, S. V. *Macromolecules* **1997**, *30*, 4520.
(12) Pugh, C.; Shao, J.; Ge, J. J.; Cheng, S. Z. D. *Macromolecules* **1998**, *31*, 1779.
(13) Delaude, L.; Jan, D.; Simal, F.; Demonceau, A.; Noels, A. F. *Macromol. Symp.* **2000**, *153*, 133.
(14) Kim, G. H.; Pugh, C.; Cheng, S. Z. D. *Macromolecules* **2000**, *33*, 8983.
(15) Oh, S. Y.; Akagi, K.; Shirakawa, H.; Araya, K. *Macromolecules* **1993**, *26*, 6203.
(16) Gato, H.; Akagi, K.; Shirakawa, H.; Oh, S. Y.; Araya, K. *Synth. Met.* 1995, *71*, 1899.
(17) Akagi, K.; Shirakawa, H. *Macromol. Sym.* **1996**, *104*, 137.
(18) Yoshino, K.; Kobayashi, K.; Myojin, K.; Ozaki, M.; Akagi, K.; Gato, H.; Shirakawa, H. *Jpn. J. Appl. Phys.* **1996**, ***35***, 3964.
(19) Dai, X. M.; Gato, H.; Akagi, K.; Shirakawa, H. *Synth. Met.* **1999**, *102*, 1289.
(20) Tang, B. Z.; Kong, X.; Wan, X.; Feng, X. D. *Macromolecules* **1997**, *30*, 5620.

(21) Tang, B. Z.; Kong, X.; Wan, X.; Peng, H.; Lam, W. Y.; Feng, X. D.; Kwok, H. S. *Macromolecules* **1998**, *31*, 2419.
(22) Kong, X.; Tang, B. Z. *Chem. Mater.* **1998**, *10*, 3352.
(23) Kong, X.; Lam, W. Y.; Tang, B. Z. *Macromolecules* **1999**, *32*, 1722.
(24) Lam, W. Y.; Kong, X.; Dong, Y.; Cheuk, K. L.; Xu, K.; Tang, B. Z. *Macromolecules* **2000**, *33*, 5027.
(25) Huang, Y. M.; Lam, J. W. Y.; Cheuk, K. K. L.; Ge, W.; Tang, B. Z. *Macromolecules* **1999**, *32*, 5976.
(26) Huang, Y. M.; Lam, J. W. Y.; Cheuk, K. K. L.; Ge, W.; Tang, B. Z. *Thin Solid Films* **2000**, *363*, 146.
(27) Huang, Y. M.; Ge, W.; Lam, J. W. Y.; Tang, B. Z. *Appl. Phys. Lett.* **2001**, *78*, 1652.
(28) Hsu, C. H.; Lu, Y. H. *J. Polym. Sci., Polym. Chem. Ed.* **1991**, *29*, 977.
(29) Lu, Y. H.; Hsu, C. H. *Macromolecules* **1995**, *28*, 1673.
(30) Simionescu, C. I.; Percec, V.; Dumitrescu, S. *J. Polym. Sci., Polym. Chem. Ed.* **1977**, *15*, 2497.
(31) Simionescu, C. I.; Percec, *V. J. Polym. Sci., Polym. Symp.* **1980**, *67*, 43.
(32) Matsunami, S.; Kakuchi, T.; Ishii, F. *Macromolecules* **1997**, *30*, 1074.

MA0107962